Journal of the European Ceramic Society 20 (2000) 2047–2054

Preparation of dense $La_{0.7}Ca_{0.3}MnO_3$ ceramics from freeze-dried precursors

O.A. Shlyakhtin [a,b], Young-Jei Oh [a,*], Yu.D. Tretyakov [b]

[a] *Materials Science and Technology Division, Korea Institute of Science and Technology, PO Box 131, Cheongryang, Seoul 130-650, South Korea*
[b] *Department of Chemistry, Moscow State University, 119899 Moscow, Russia*

Received 10 January 2000; received in revised form 24 February 2000; accepted 26 February 2000

Abstract

Sinterability of $La_{0.7}Ca_{0.3}MnO_3$ precursors, obtained by the freeze-drying method, is studied in order to develop a technique for preparation of dense (>95%) ceramics for CMR measurements and sputtering applications. Single phase powders, obtained by thermal decomposition at 650°C, were subjected to deagglomeration by ultrasonic or mechanical treatment. Sintering of deagglomerated powders for several hours at $T = 1200$–1300°C allowed to achieve densities up to 97–98%. The best sinterability is demonstrated by mechanically processed powder, but further sintering of ceramics, obtained from this precursor, results in significant dedensification (up to 85% at 1300°C). Analysis of precursors and dedensified samples shows at high temperature decomposition of carbonates in closed pores to be the most probable reason for the observed process.

Keywords: (La,Ca)MnO_3; Perovskites; Porosity; Powders-chemical preparation; Sintering

1. Introduction

The recent discovery of colossal magnetoresistance in perovskite complex oxides resulted in a number of new applications of these materials.[1] The most significant of them until now are thin-film devices, while a large number of these films are prepared by the laser ablation method. It makes feasible the development of techniques for preparation ceramic sputtering targets in order to ensure planar and spatial homogeneity of ablated films. Features of the laser ablation method set some specific demands for ceramic samples being used as sputtering targets, first of all, the maximum chemical homogeneity and minimum porosity of used material.

The preparation of manganite ceramics is mentioned in several papers devoted to the study of magnetoresistive properties of perovskite CMR materials.[2–4] The details of dense material preparation from manganite powders were not usually considered; in most cases the density or any other parameters of prepared materials are not mentioned at all. At the same time, more detailed study of densification processes may be important not only for optimization of target preparation processes. While the CMR effect in high (several Tesla) magnetic fields is controlled mostly by crystallochemical features of a particular phase,[5] the effects in smaller fields are strongly related to the microstructure of the powder, ceramic or thin film samples.[6] Some papers refer to the significant enhancement of CMR ratio in polycrystalline samples compared to single crystals or epitaxial films,[7,8] while properties of high density CMR ceramics remain underestimated. These considerations give additional reasons to study the sintering processes of fine powders of La–Ca manganite. The freeze-drying method demonstrated its efficiency in obtaining many other similar dense ceramic materials,[9] and has been selected for precursor powder preparation.

2. Experimental

A stock solution for freeze-drying (FD) synthesis was prepared by mixing of appropriate amounts of preanalyzed 0.3–0.5 M solutions of La and Mn acetates and Ca nitrate. The solution was sprayed by pneumatic nozzle (mean diameter of droplet = 100–200 μm) into liquid nitrogen under intensive stirring, then tray-dried in a semi-industrial freeze-drier SMH-15 (Usifroid) at

* Corresponding author.

0955-2219/00/$ - see front matter
PII: S0955-2219(00)00080-7

$P = 4 \times 10^{-2}$ mBar for 48 h; the temperature of the heating plates was changed from −50 to +40°C. Thermal decomposition of salt powders, obtained by freeze-drying, was performed by slow heating (l K/min) of the powder in air up to 650°C with a further 5 h annealing.

Solid state (SS) synthesis of reference samples was performed by ball-milling of MnO_2, La_2O_3 and $CaCO_3$, taken in the stoichiometric ratio, with ZrO_2 balls in ethanol for 24 h followed by annealing for 40 h in air at 1000°C and for 20 h at 1150°C in air with intermediate grinding. In order to avoid the appearance of secondary phases due to crystallization during sintering, additional heat treatment at 1300°C for 10 h was applied to several samples.

To study the influence of aggregates/agglomerates on the sintering process, two types of deagglomeration procedures have been applied. During ultrasonic (US) treatment, oxide powder has been subjected to intensive US treatment in water, containing 0.5% of isobuthanol. In order to prevent reagglomeration during suspension media removal, US treated slurry was subjected to freeze-drying. Mechanical deagglomeration/disaggregation of samples was realized by ball-milling with ZrO_2 balls in ethanol for 1 day followed by air drying; 5% of PVA binder was added before pressing the powders. The density of pellets was measured by geometrical method and by hydrostatic weighing in absolute ethanol ($\rho = 0.79$ g/ml). Measurements of aggregate/agglomerate size in powders was performed in centrifugal particle size analyzer SA-CP2; elimination of weak agglomerates was realized by ultrasonic treatment in 0.2% aqueous solution of $Na_2P_2O_7$. SEM studies were performed on powders, attached to conducting tape and coated with a thin film of gold, and on fractured surfaces of as-obtained sintered ceramic samples, also coated with gold film.

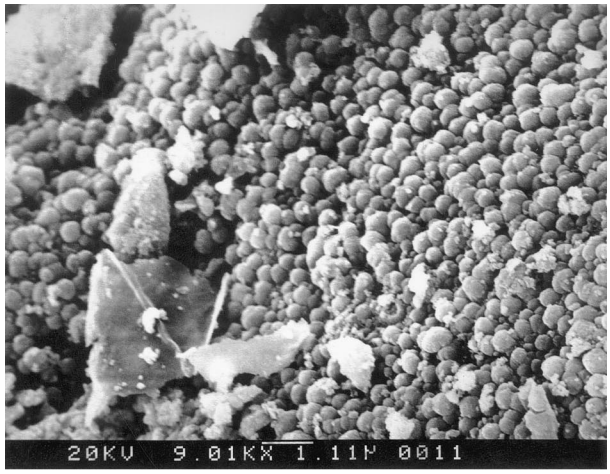

(a)

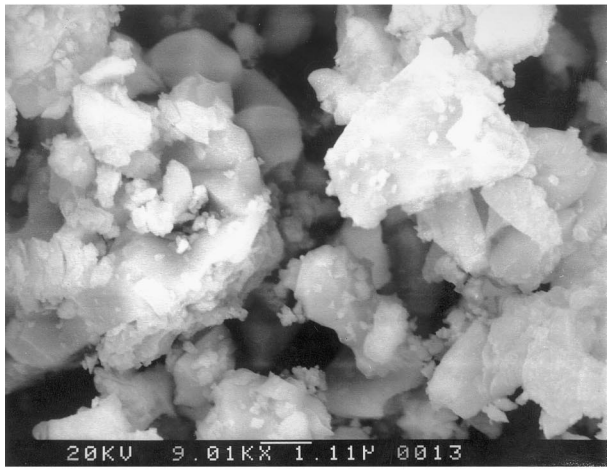

(b)

Fig. 1. SEM micrographs of $La_{0.7}Ca_{0.3}Mn_{0.3}$ powders, obtained by (A) freeze-drying and (B) solid state synthesis methods.

2.1. Powder processing and properties

Thermal analysis curves of the freeze-dried salt precursor (Q-1500 thermoanalyzer, air, 10 K/min) demonstrate that thermal decomposition is completed at 620°C. Usually, thermal decomposition of freeze-dried salt precursors in multicomponent systems is accompanied by formation of complex oxide phases,[9] but they are often amorphous or poorly crystalline. In order to ensure better accuracy of XRD control, thermal decomposition of freeze-dried samples was performed at 650°C, with additional annealing at this temperature. XRD analysis of the powder product confirmed the formation of single-phase $La_{0.7}Ca_{0.3}MnO_3$ (LCM). Single phase LCM samples were obtained also by the solid state method, though the observed rate of phase formation in that case was much lower in spite of substantially higher synthesis temperatures. SEM analysis of both powders demonstrates substantial difference in the size of crystallites according to various temperatures of phase formation (Fig. 1).

Along with the size of crystallites, another microstructural parameter determining the sinterability of powders is spatial arrangement of crystallites, which can be described both in terms of size distribution of pores and aggregates/agglomerates. It is well known that a higher rate of sintering is observed for precursors with spatially more "uniform" microstructure, with comparable distances between crystallites belonging to the same and to different clusters (aggregates). The typical microstructure of freeze-dried powders is far from this model due to micron-sized voids, left by water during freeze-drying, retained during the following thermal decomposition and formation of complex oxide.[9] For phases/materials with melting temperature < 1800°C, like $La_{0.7}Ca_{0.3}MnO_3$ this factor is usually not so important: their sintering in most cases proceeds in the bulk diffusion regime, which allows healing of the pores within reasonable time. Nevertheless, breaking the aggregates (elimination of large pores) is usually efficient for sinterability enhancement of these materials too.

Both applied deagglomeration procedures, ultrasonic treatment and ball-milling, had no significant influence on the size of powder crystallites. As for deagglomeration efficiency, the difference between these procedures is clearly visible by SEM (Fig. 2): ultrasonic treatment results in breaking only the weakest agglomerates, while milling destroys almost all structures up to primary (crystallite) level. More quantitatively, it can be illustrated by centrifugal particle size analysis data, which are less influenced by residual weak agglomeration (Fig. 3): US treatment results in a decrease in the number of the biggest agglomerates and an increase in the amount of submicron particles, without substantial influence on the basic distribution mode. Apart from US, mechanical milling is accompanied by total rearrangement of aggregate structure, with shifting of the center of distribution to the submicron level.

The influence of deagglomeration on the density of the green body is not so significant: it grows from 52 to 53% for original FD powder to 54 to 55% for US-deagglomerated and to 56 to 57% for ball-milled LCM powder. Apart from FD powders, the green density of pellets from SS powders is much higher — up to 70%. Such a difference in the green densities of FD and SS powders is more or less typical for oxide powders, obtained by solid state and wet chemical methods. Significant shrinkage of the green bodies, obtained by pressing FD powders, is observed at $T \geqslant 1000^{\circ}C$. Nevertheless, density values over 90% of theoretical can be achieved within reasonable time only at $T = 1200^{\circ}C$ or higher.

2.2. Sintering: influence of powder microstructure

The results of isothermal sintering runs, performed in air at heating rate 5 K/min followed by dwelling for 0.1–90 h, demonstrate the significant influence of deagglomeration on the sintering behavior of FD powders: both US- and mechanically-treated FD samples are densified

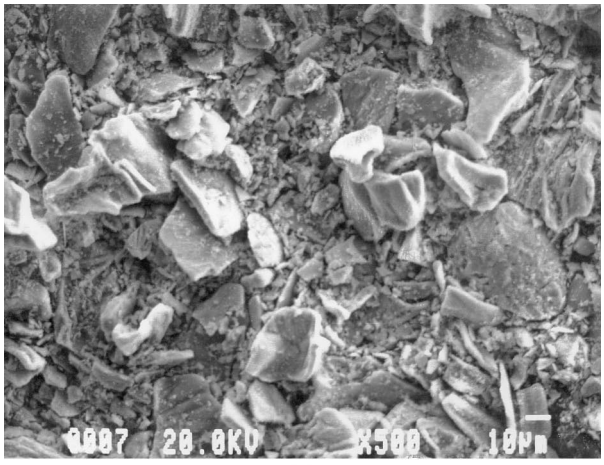

(a)

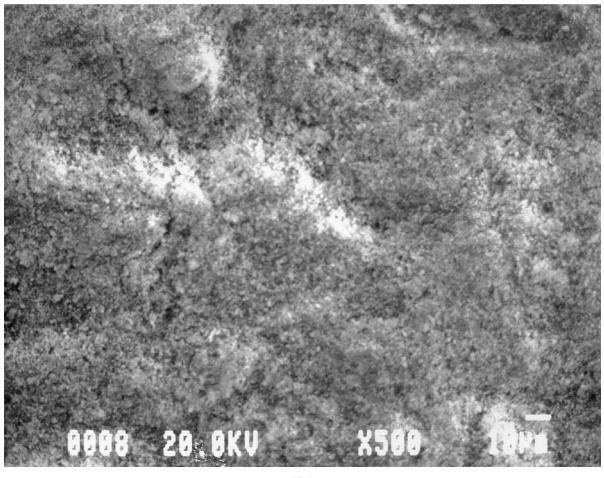

(b)

Fig. 2. SEM micrographs of freeze-dried $La_{0.7}Ca_{0.3}MnO_3$ powder, subjected to: (A) ultrasonic deagglomeration; (B) ball-milling.

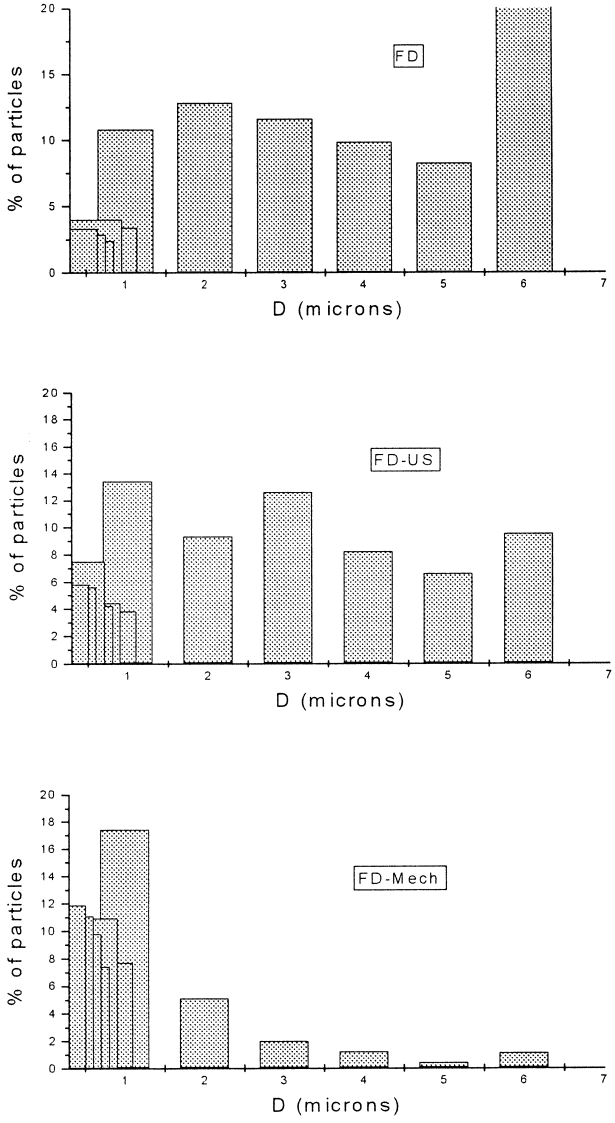

Fig. 3. The data of aggregate/agglomerate size analysis of precursor powders by centrifugal sedimentation method.

up to 92–95% just in the course of heating up to sintering temperature even at 1200°C (Fig. 4a). Further sintering of US sample leads to even higher densities, but the rate of this process is much slower than at the initial stage. Such a behavior correlates with the mechanism of viscous flow of deforming particles and some kind of separation of compaction and grain growth stages of the sintering process. Shrinkage of conventional (aggregated) FD compact is made much more complicated by bridges between crystallites, but even in this case the sintering curve demonstrates the possibility of attaining high density values at longer sintering times.

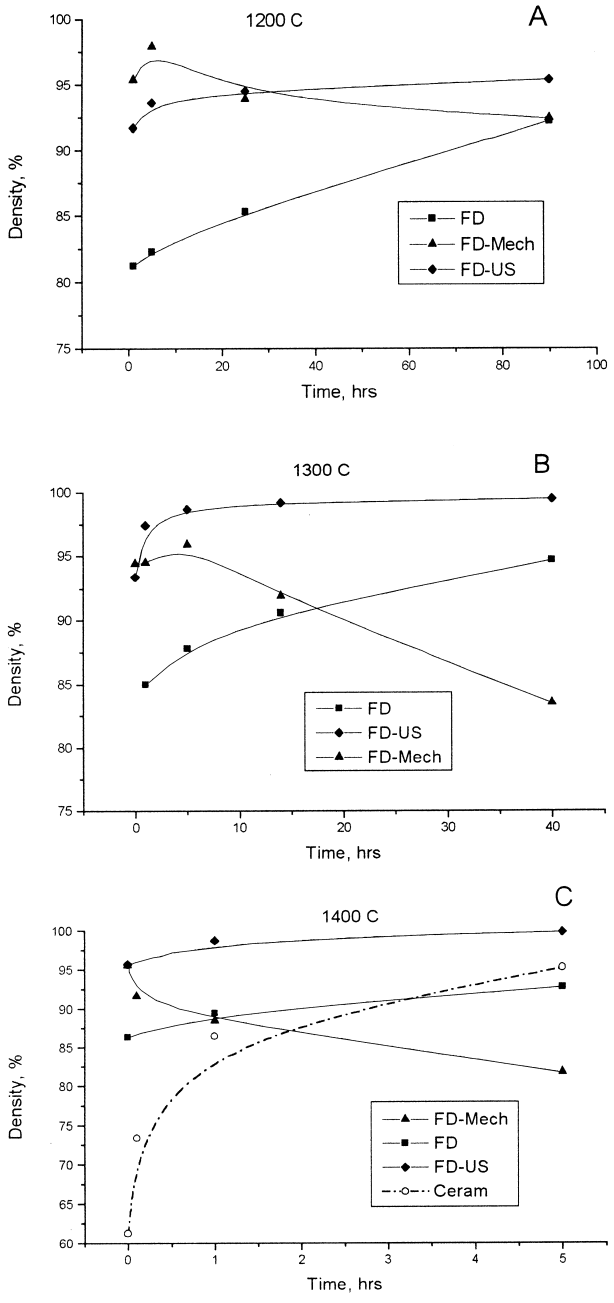

Fig. 4. Densification curves of ceramics (geometric method), prepared from various precursors, at different sintering temperatures. FD = freeze drying synthesis; Ceram = solid state synthesis; US = ultrasonic deagglomeration; Mech = mechanical processing by ball-milling.

Sintering at 1300°C (Fig. 4b) seems to be more attractive from the practical point of view. Dwelling of US-treated samples for 5 h or more allows to obtain ceramics with density over 97%. The values of the density, obtained by the sample dimensions measurement method, correspond quite well to those obtained by the hydrostatic method, and demonstrate good reproducibility in repeated sintering runs. This density, achieved by conventional free sintering, appears to be enough for practical purposes; moreover, several samples obtained during these experiments demonstrated densities close to theoretical value. Such a behavior is not typical for oxide powders with FD prehistory[9] and shows the greater potential possibilities of this method in ceramics preparation.

The difference of sinterability between FD and SS samples is predictable, taking into account the different initial size of LCM crystallites (Fig. 1). At the same time, the sintering activity of SS powder is large enough to achieve the density about 95% for several hours at 1400°C so that a further increase of sintering temperature might lead to an even smaller difference between FD and SS powders behavior. The most significant differences of ceramics obtained from SS and FD precursor powders deal with various reoxidation rate of dense samples during cooling of samples and related colossal magnetoresistance (CMR) properties. These features, as well as the dynamics of CMR properties in the course of sample densification, are described in more detail elsewhere[10].

A substantial change of sintering behavior of FD powder by deagglomeration can be clearly illustrated by opposing tendencies of closed porosity dynamics during sintering (Fig. 5). Conventional FD samples demonstrate enhancement of closed porosity, which actually should be attributed to rearrangement of initially open pores into closed ones, while total porosity continues to decrease (see Fig. 4). The opposite behavior of closed porosity in deagglomerated samples is related to almost total elimination of the open porosity at the very beginning of sintering due to noncomplicated sliding of primary crystallites. Hence, the process of further densification in such a case is equivalent to the slow elimination of the closed porosity.

2.3. Dedensification studies

Another important phenomenon, observed during these studies, was substantial dedensification of the mechanically deagglomerated body during sintering. It was rather unexpected, taking into account that usually deagglomeration results in enhancement of sinterability and, hence, higher density values compared to untreated samples. It was true only for the initial sintering period (~5 h at 1200–1300°C; Fig. 4a and b). Further sintering of mechanically deagglomerated samples was accompanied

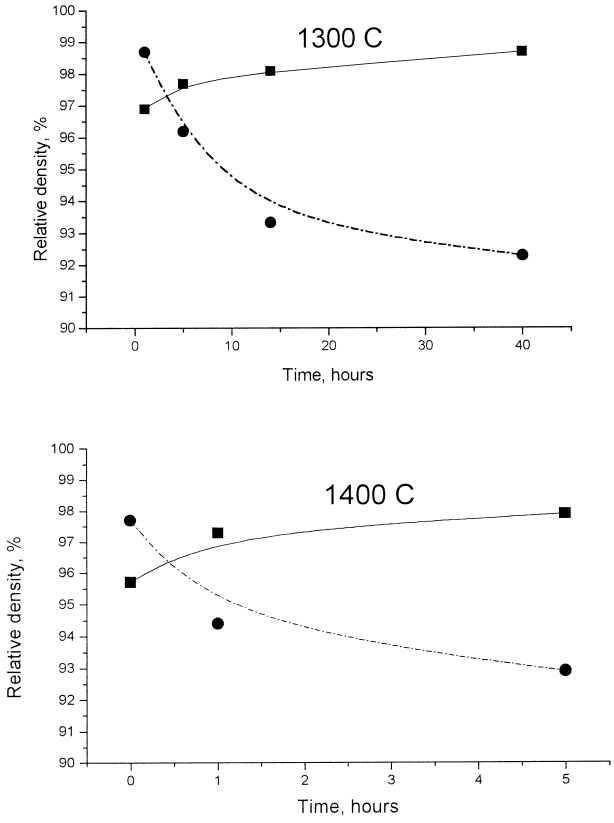

Fig. 5. Dynamics of density, measured by Archimede's method, during sintering at different temperatures FD (dashed line) and US-FD (solid line) precursors.

by continuous density decrease, especially pronounced at 1300°C.

The reasons for such behavior, also known as swelling and observed by many authors, can be divided into three main groups. The first group of reasons are clearly related to the chemical nature of the components in the multiphase materials (alloys, oxide and metal oxides composites, etc.) and connected with formation in the dense compact of the new phase (oxide, complex oxide) with greater specific molar volume,[11,12]. Similar reasons may cause dedensification if one of the system components undergoes phase transformation during sintering. Nevertheless, both reasons are poorly applicable to dedensification of single phase manganites, demonstrating no phase transitions in the studied temperature intervals.

Secondly in a large number of single phase ceramic materials the dedensification is usually attributed to secondary crystallization or exaggerated grain growth.[13] In that case, large grains, growing in the matrix of primary crystallites, form a continuous network which, in turn, creates internal tensile stresses in the sample body, causing microcracking and formation of new pores. Due to this mechanism, a typical attribute of this kind of dedensification process is the appearance of large grains in the matrix of small crystallites. As the exaggerated grain growth itself, dedensification of this type is enhanced by

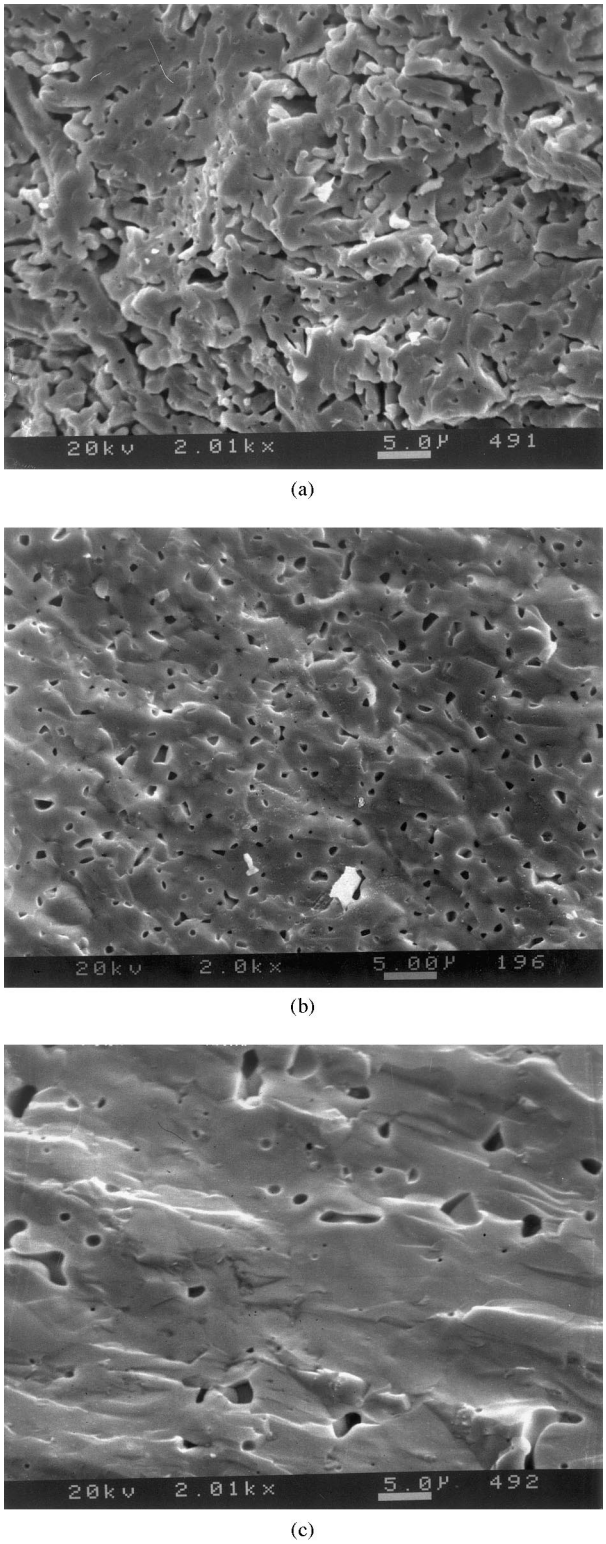

Fig. 6. SEM micrographs of ceramics, obtained by sintering at 1300°C for 1 h (a) FD precursor; (b) FD-Mech precursor; (c) FD-US precursor.

some dopants,[14,15] promoting the formation of eutectic melts at grain boundaries and, hence, accelerating grain boundary diffusion. The dopant phases can be introduced intentionally, or may appear as a result of partial

melting or decomposition of matrix phase,[14] and are usually detectable at grain boundaries by EDX control.

The third group of phenomena causing dedensification is related to formation of gases (O_2, CO_2, SO_2, etc.) due to high temperature decomposition processes.[16–18] If such a formation proceeds within a dense ceramic body with a small number of open pores, a large (up to several MPa[16]) internal pressure of non-diffusive gases, released in closed pores, causes expansion of the last ones and, hence, substantial reduction of total density of the sample. Hence, attributes of this mechanism are the close correlation of total and closed porosity of the sample, and the existence of components which decompose until sintering temperatures.

Given these reasons, some additional studies have been performed in order to study the possible reasons for dedensification for LCM ceramics. SEM studies of $La_{0.7}Ca_{0.3}MnO_3$ samples, obtained by sintering various precursors, demonstrated drastic differences in their microstructure, which correlate quite well with observed density values and processing prehistory. Moderate sinterability of the native cryochemical $La_{0.7}Ca_{0.3}MnO_3$ precursor is explained by keeping the aggregates, presented in the precursor powder, at the initial stages of sintering (Fig. 6a). Even the low-energy breaking of the upper-level aggregates by ultrasonic treatment results in much better packing of crystallites and the formation of a rather dense ceramic matrix; observed voids probably correspond to former interagglomerate pores (Fig. 6c). The appearance of a large number of small pores in the ball-milled sample (Fig. 6b) can be explained by simultaneous enhancement of grain growth processes, resulting in earlier formation of larger and, hence, less mobile particles. Another reason, relative to probable gas evolution, will be considered further.

The microstructure of samples at succeeding stages of sintering also demonstrates the development of tendencies observed during primary densification. Densification of the native cryochemical sample is accompanied by systematic healing of interagglomerate pores (Fig. 7a). Sintering of a US-processed sample demonstrates Ostwald's ripening of porosity, when final densification is accompanied by growth of largest residual pores (Fig. 7c). The only sample, different from other two precursors and demonstrating clearly distinguished granular structure, is the mechanically deagglomerated one (Fig. 7b). Nevertheless, the observed type of grain size distribution is unlikely to be considered as a reason for dedensification processes, due to no clear evidence of bimodal grain size distribution and formation of the outgrown grains network.

Further microprobe studies of element concentration profiles by EDX demonstrated no compositional fluctuations at grain boundaries as well as the absence of impurities which may cause anomalous crystallization or grain growth. Total average compositions of samples with various prehistories are also indistinguishable, so that non-stoichiometry- or impurity-related reasons for densification should be considered as the least probable.

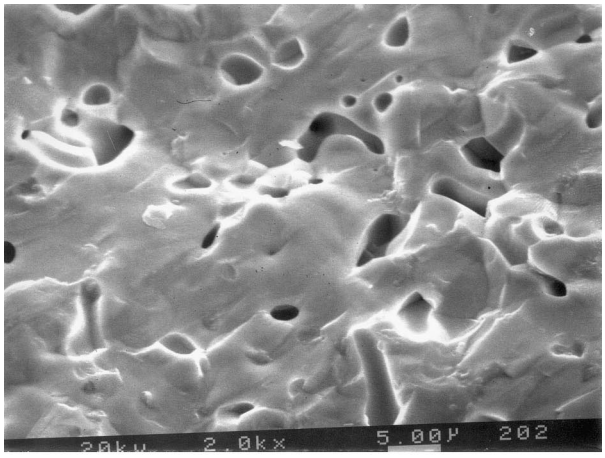

(a)

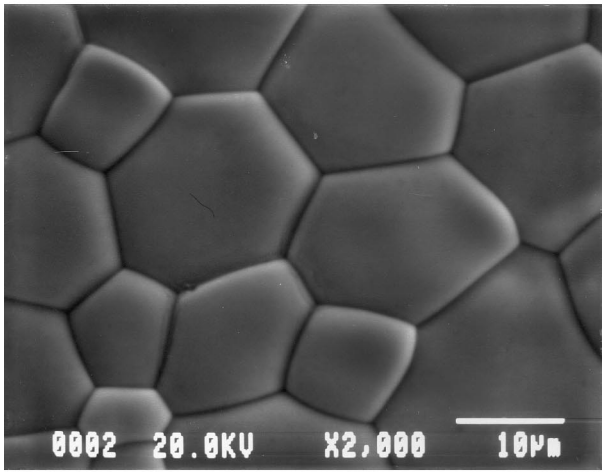

(b)

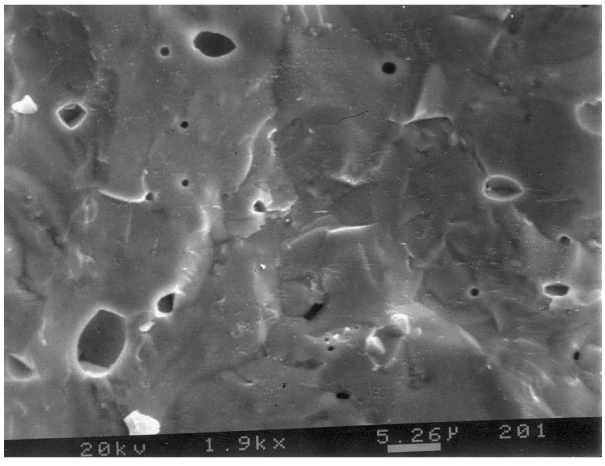

(c)

Fig. 7. SEM micrographs (×2000) of ceramics, obtained by sintering at 1300°C for 40 h. (a) FD precursor; (b) FD-Mech precursor; (c) FD–US precursor.

The only probable reason left for the dedensification is expansion of closed porosity due to gas release.

This model finds much better agreement with experimental data. First of all, samples obtained by sintering of ball-milled precursor have almost no open porosity at both densification and dedensification branches of sintering curves (Fig. 8). It would be difficult to attribute this feature to any other dedensification model, where at least a small number of new open pores should appear. Thermogravimetric analysis (Fig. 9) also demonstrated a reproducible and substantial difference between native cryochemical and mechanically deagglomerated precursor, i.e. continuous weight loss, occurred until $T \geqslant 1400°C$ even at low heating rates (2 K/mm). The evolving of gas from ball-milled samples is confirmed also by the appearance of bubbles at their surface after sintering at 1400°C, similar to cavities at dedensified tetragonal ZrO_2.[16] The liberation of this gas within the dense sample at the temperatures, when the diffusion mobility of the constituents is high enough, should lead to the appearance of new pores and their growth due to the previously mentioned Ostwald's ripening process. Experimentally, such a phenomenon should be observed as intensive enhancement of closed porosity with little or no influence at the open pores, which is actually observed in our studies (Fig. 8).

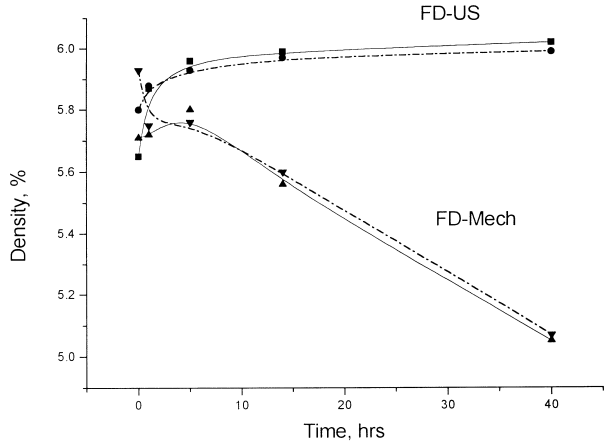

Fig. 8. Relative behaviour of total and closed porosity during sintering of ceramics from various precursors at 1300°C. Solid lines = density, measured by geometric method; dashed lines = density, measured by Archimedes' method.

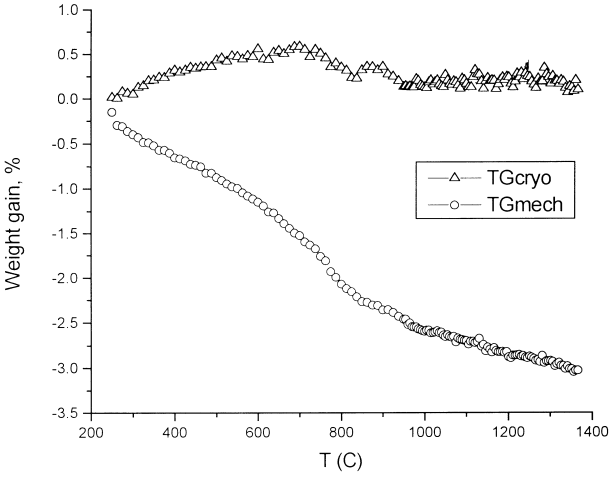

Fig. 9. TG curves of FD and FD-Mech precursor powders (air; heating rate = 2 K/mm).

Analysis of the composition of the evolved gas was not performed, but the most probable reason for this weight loss is CO_2 evolution. Substantial destabilization of oxygen sublattice by low energy ball-milling does not seem to be probable; moreover, evolved oxygen might escape from closed pores due to significant oxygen non-stoichiometry of $La_{0.7}Ca_{0.3}MnO_3$ at sintering temperatures.[10] At the same time, many La- and Sr-containing complex oxides readily react with atmospheric CO_2. especially after mechanical activation. This interpretation is confirmed also by high temperatures of thermal decomposition of Sr carbonate and, especially, La oxycarbonate (>930°C at atmospheric pressure); trace amounts of the latter can be kept in closed pores until quite high temperatures.

3. Conclusions

It should be noted that submicron manganite powders, prepared by the freeze drying method, demonstrated excellent activity in the process of free sintering, large enough to obtain ceramics with density over 97% at reasonable temperatures (1300°C). The character of sintering curves and their variation for powders with various prehistory and microstructure show the possibility of further enhancement of sinterability by means of optimization of processing conditions. At the same time, the present work is devoted to the sintering of $La_{0.7}Ca_{0.3}MnO_3$, being only one of the large manganite CMR materials family. Other members of this series might have their own features related to their structural and thermodynamic properties, so that additional work is needed in order to optimize processing conditions for a particular CMR phase.

Another important conclusion concerns more careful application of mechanical activation during processing of CMR manganites. Observed dedensification phenomena can be only one of the manifestations of atmospheric degradation processes in these materials, which obviously need more careful investigation in order to avoid more serious problems during their practical application.

Acknowledgements

The work is supported by Korea Institute of Science and Technology Evaluation and Planning (KISTEP) grant. O.A. Shlyakhtin is grateful to V.V. Ischenko (MPI Stuttgart) for his kind help and fruitful discussion.

References

1. Daughton, J. M., GMR applications. *J. Magn. Magn. Mater*., 1999, **192**, 334–342.
2. Hueso, L. E., Rivadulla, F. and Sanchez, R. D., Influence of the grain size and oxygen stoichiometiy on magnetic and transport properties of polycrystalline $La_{0.67}Ca_{0.33}MnO_{3\pm\delta}$ perovskites. *J. Magn. Magn. Mater*., 1998, **189**, 321–328.
3. Wang, X. L., Dou, S. X. and Liu, H. K., Large low-field magneto resistance over a wide temperature range induced by weak-link grain boundaries in $La_{0.7}Ca_{0.3}MnO_3$. *Appl. Phys. Lett*., 1998, **73**(3), 396–398.
4. Shim, In-Bo, Bae, Seung-Young, Oh, Young-Jei and Choi, Se-Young, Magnetic inhomogeneity in colossal magnetoresistive $La_{0.7}Ca_{0.3}MnO_3$ perovskite ceramics. *Solid State Jonics*, 1998, **108**, 241–247.
5. Mahesh, R., Mahendiran, R., Raychaudhuri, A. K. and Rao, C. N. R., Effect of the internal pressure due to the A-site cations on the giant magnetoresistance and related properties of doped rare earth manganates, $Ln_{1-x}A_xMnO_3$ (Ln = La,Nd,Gd,Y;A = Ca, Sr, Ba, Pb). *J. Solid State Chem*., 1995, **120**, 204–208.
6. Hwang, H. Y., Cheong, S.-W., Ong, N. P. and Batlogg, B., Spin-polarized intergrain tunneling in $La_{2/3}Sr_{1/3}MnO_3$. *Phys. Rev Lett*., 1996, **77**, 2041.
7. Shreekala, R., Rajeswari, M. and Ghosh, K., Effect of crystallimity on the magnetoresistance in perovskite manganese oxide thin films. *Appl. Phys. Lett*., 1997, **71**(2), 282–284.
8. Ranno, L., Llobet, A., Hunt, M. B. and Pierre, J., Influence of substrate temperature on magnetotransport properties of thin films of $La_{0.7}Sr_{0.3}MnO_3$. *Appl. Surf. Sci*., 1999, **138–139**, 228–232.
9. Tretyakov, Yu, D., Oleynikov, N. N. and Shlyakhtin, O. A., *Cryochemical Technology of Advanced Materials*. Chapman & Hall, London, 1997.
10. Shlyakhtin, O. A., Oh, Young-Jei and Tretyakov Yu, D., Influence of thermal and chemical prehistory on the colossal magnetoresistance of $La_{0.7}Ca_{0.3}MnO_3$ ceramics. *Solid State Comm*., 1999, **111**(12), 711–715.
11. Rocaniere, C., Dehaudt, P. and Gaudreau, B. Oxidizing sintering behaviour of UO_{2+x}-lanthanide oxide compounds. *Key Engineering Materials*, 1997, **132–136**(2), 916–919.
12. Wang, H. A., Kroeger, F. A. Pore formation during oxidative annealing of Al_2O_3-Fe and slowing of grain growth by precipitates and pores. *J. Mater. Sci*., 1983, **13**, 1978–1986.
13. Kingery, W. D., Bowen, H. K., Uhlmann, D. R. *Introduction to Ceramics*. John Wiley, New York, 1973, pp. 461–468.
14. Demartin, M., Herard, C., Carry, C. and Lemaitre, J., Dedensification and anomalous grain growth during sintering of undoped barium titanate. *J. Am. Ceram. Soc*., 1997, **80**(5), 1079–1084.
15. Moriyoshi, Y., Shimizu, Y., Tanaka, H., Ekinaga, N. and Ikegami, T., Impurity precipitation along grain boundaries in sintered alumina. *J. Mat. Synth. Proc*., 1998, **6**(4), 261–266.
16. Smith, A. and Baumard, J.-F., Sinterability of Tetragonal ZrO_2 Powders. *Am. Ceram. Soc. Bull*., 1987, **66**(7), 1144–1148.
17. Descemond, M., Brodhag, C., Thevenot, F., Durand, B., Roubin, M. and Samdi, A., Influence of production conditions on the densification of zirconia powders obtained from acetates. *J. Mat. Sci*., 1993, **28**, 3754–3760.
18. Lorrain, N., Chaffron, L. and Carry, C., Sintering and evolution of the microstructure of nanocomposite powders Ag–SnO_2 prepared by reactive milling. *Mater. Sci. Forum*, 1999, 312–314, 153–158 (Metastable, Mechanically Alloyed and Nanocrystalline Materials).